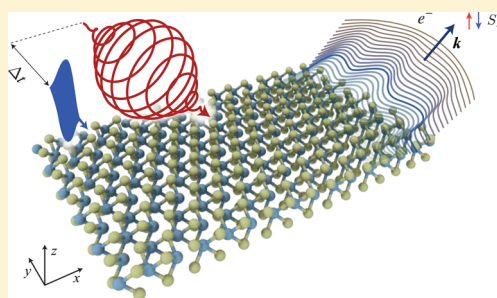


Monitoring Electron-Photon Dressing in  $\text{WSe}_2$ Umberto De Giovannini,<sup>†,‡,§,||</sup> Hannes Hübener,<sup>†</sup> and Angel Rubio<sup>\*,†,§,||</sup><sup>†</sup>Nano-Bio Spectroscopy Group, University of the Basque Country UPV/EHU, Avenida de Tolosa 72, 20018 San Sebastian, Spain<sup>‡</sup>Dipartimento di Fisica e Chimica, Università degli Studi di Palermo, Via Archirafi 36, I-90123, Palermo, Italy<sup>§</sup>Max Planck Institute for the Structure and Dynamics of Matter, Luruper Chaussee 149, 22761 Hamburg, Germany<sup>||</sup>Center for Free-Electron Laser Science and Department of Physics, University of Hamburg, Luruper Chaussee 149, 22761 Hamburg, Germany

## Supporting Information

**ABSTRACT:** Optical pumping of solids creates a nonequilibrium electronic structure where electrons and photons combine to form quasiparticles of dressed electronic states. The resulting shift of electronic levels is known as the optical Stark effect, visible as a red shift in the optical spectrum. Here we show that in a pump–probe setup we can uniquely define a nonequilibrium quasiparticle bandstructure that can be directly measurable with photoelectron spectroscopy. The dynamical photon-dressing (and undressing) of the many-body electronic states can be monitored by pump–probe time and angular-resolved photoelectron spectroscopy (tr-ARPES) as the photon-dressed bandstructure evolves in time depending on the pump–probe pulse overlap. The computed tr-ARPES spectrum agrees perfectly with the quasi-energy spectrum of Floquet theory at maximum overlap and goes to the equilibrium bandstructure as the pump–probe overlap goes to zero. Additionally, we show how this time-dependent nonequilibrium quasiparticle structure can be understood to be the bandstructure underlying the optical Stark effect. The extension to spin-resolved ARPES can be used to predict asymmetric dichroic response linked to the valley selective optical excitations in monolayer transition metal dichalcogenides (TMDs). These results establish the photon dressed nonequilibrium bandstructures as the underlying quasiparticle structure of light-driven steady-state quantum phases of matter.



**KEYWORDS:** First-principles calculations, photoelectron spectroscopy, nonequilibrium bandstructure, pump–probe spectroscopy, Floquet theory

Laser driving of solids is believed to give rise to a steady-state nonequilibrium phase of the electronic structure where quasiparticles of combined photons and electrons emerge with a distinct band structure, so-called Floquet–Bloch bands.<sup>1</sup> At off-resonant driving, the energy of the photons is not absorbed by electronic states but instead they dress the electronic structure via virtual photon processes, leading to distinctive replica bands at multiples of the driving energy. These photon-dressed electronic states can have dramatically different properties from those of their equilibrium counterparts. In particular the possibility to induce topological phases on an ultrafast time-scale has received much attention recently, following the proposal of a Floquet-topological insulator.<sup>2</sup> In such a system, the coupling to a monochromatic light field can be used to induce, in an ordinary equilibrium semiconductor, nontrivial topological order leading to the emergence of topologically protected edge states. Similar mechanisms have been proposed to engineer the topology in 2D Dirac materials.<sup>3–6</sup> Early on it was realized that the Floquet mechanism can also be used to create solid state versions of the elusive Majorana Fermions<sup>7–9</sup> that have still not been directly observed. With the discovery of bulk Dirac semimetals<sup>10,11</sup> the scope for Floquet materials has considerably

widened and in particular the creation of nonequilibrium Floquet–Weyl Fermions has been discussed.<sup>12–14</sup> Other recent Floquet-topological phenomena include nodal rings,<sup>15</sup> type-II Floquet–Weyl semimetals,<sup>16</sup> carbon nanotubes,<sup>17</sup> and sound-waves<sup>18</sup> among others.

While this shows how the number of theoretical proposals for Floquet-topological phenomena is currently growing at a fast pace, experimental evidence for the existence and measurability of the underlying Floquet-bandstructure is somewhat lacking. Only two recent experiments unambiguously found direct proof of Floquet states on the surface of a topological insulator via tr-ARPES spectroscopy.<sup>19,20</sup> Yet, it is commonly assumed that such bands appear in any kind of material and particularly in the bulk phase. Tr-ARPES is the method of choice for monitoring many groundstate and excitation phenomena in solids, giving access to the time-dependent development of spatial, momentum and spin degrees of freedom of single energy levels. In this work, we use first-principles computational techniques to show under

Received: October 21, 2016

Revised: November 23, 2016

Published: November 23, 2016

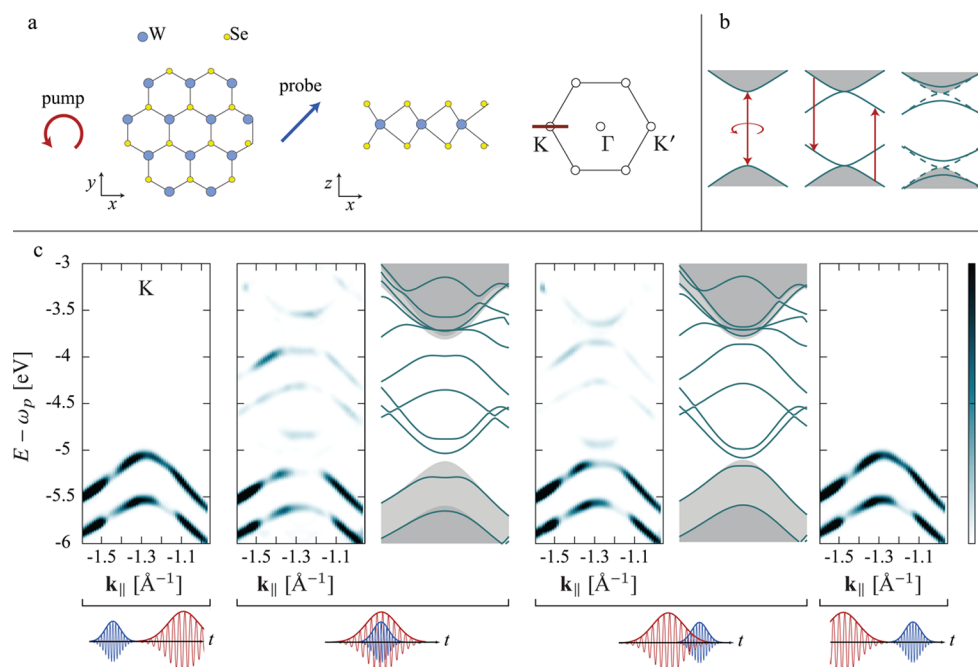


**Figure 1.** Dressing and undressing. (a) The  $\text{WSe}_2$  monolayer is aligned with the  $x$ – $y$  plane as is the polarization plane of the circularly polarized pump pulse (red). The probe pulse (blue) is linearly polarized in the  $x$ – $z$  direction and the photoelectron spectrum is computed on a short path in the Brillouin zone crossing  $K$  in the  $K$ – $\Gamma$  direction. (b) Scheme illustrating the hybridization of photon-dressed bands induced by driving a semiconductor at resonance with its band gap. (c) tr-ARPES spectra obtained by varying the delay between the pump (red) and the probe (blue) pulses schematically reported at the bottom. Photon-dressed bands obtained with Floquet theory are shown side-by-side for overlapping delays. The pump pulse is resonant with the band gap at 1.31 eV with a peak amplitude  $A = 5$  au/c while the probe has  $A = 3.5 \times 10^{-2}$  au/c and  $\omega_p = 40$  eV. In the spectra, photoelectron kinetic energies  $E$  are reported relative to the probe energy  $\omega_p$ .

which conditions time-resolved pump–probe ARPES can measure Floquet-bandstructures in a semiconductor and provide a protocol for observing the creation of the emerging bands in real-time. The pump pulse creates new quasiparticle states that are subsequently probed by a second pulse and depending on the time delay between the two pulses the creation and destruction of the quasiparticles is observed. This nonequilibrium bandstructure is not only underlying the Floquet-topological phenomena but is also occurring in more conventional pump–probe experiments. The formation of the new quasiparticle levels leads to a shift in the absorption energy of the pumped system, known as the optical or dynamical Stark effect.<sup>21</sup> In a recent work, optical pump–probe spectroscopy was used to demonstrate that the Stark effect can be used in TMDs to confirm selective excitations of the electronic structure in certain valleys of the conduction band.<sup>22</sup> Here, we show how this effect emerges from the Floquet-bandstructure and how the spin polarization of the valence bands results in a spin-selective interaction of the dressed quasiparticle states.

We stress that in this work we use two different theoretical approaches based on time-dependent density functional theory (TDDFT).<sup>23</sup> We directly simulate the ARPES measurement of a pumped system by computing the time-evolution of the electronic density under presence of the two pulses and analyze the energy and momentum distribution of the ionized photoelectrons.<sup>24–26</sup> On the other hand, we perform Floquet analysis of the time evolution of the pumped system without any reference to a probe pulse but imposing periodicity in time.<sup>12</sup> The striking finding is that both methods give bandstructures that agree nearly perfectly with each other. In our simulation, we do not include coupling to lattice degrees of

freedom, which can also affect the nonequilibrium bandstructure via scattering with phonons. However, here we are considering a monolayer TMD which has a direct bandgap, so that for low excitation energies there is no significant electron–phonon scattering through the Brillouin zone. While other dissipation effect can be at play here, what we show is only the underlying electronic eigenstates of the driven system and how they emerge from the equilibrium bandstructure. A complete description of optical pumping, as suggested here, requires taking into account electron–hole interactions, which we have omitted. For the sake of clarity, we argue that the effect we discuss is generic and that it applies similarly to excitonic states. The photon-dressing mechanism that we are discussing here is not specific to  $\text{WSe}_2$  but applies to a wide range of 2D and 3D materials. For instance, it has recently been discussed that electromagnetic dressing can significantly alter the transport properties of graphene<sup>27</sup> and the 2DEG.<sup>28,29</sup>

**Dressing and Undressing of Quasiparticles.** Transition metal dichalcogenides have emerged as a platform to study many new phenomena of excited electronic structures. Their 2D stacking structure makes them particularly suitable to study monolayers where the broken inversion symmetry results in a well-defined spin texture of the valence and conduction band edge. Together with a multivalley structure of the conduction bands this property makes them particularly interesting for possible spin- and valleytronics applications.<sup>30</sup> Furthermore, the band edges have orbital-character with well-defined angular momenta so that there is a pronounced valley-selective dichroism. Recently it has been shown that also in the bulk phase most of these properties persist with each layer of the material carrying a well-defined valley-dependent spin polarization.<sup>31–33</sup> Here we consider monolayer  $\text{WSe}_2$  to utilize these

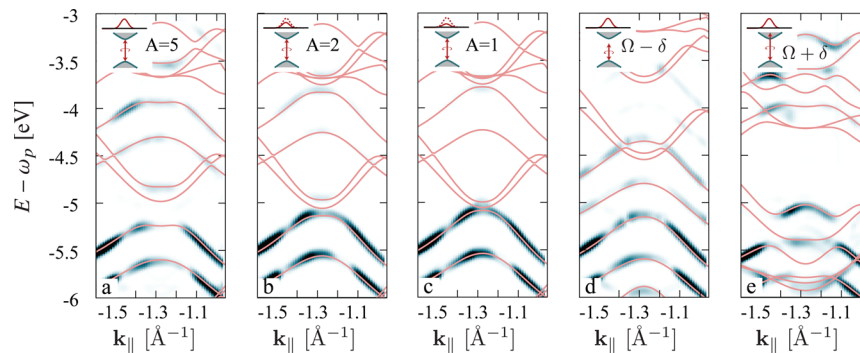


**Figure 2.** Dependence on laser parameters: vector field amplitude  $A$  and detuning  $\delta$  from the resonant band gap excitation at 1.31 eV. The amplitude and energy of the pump pulse determines the photon-dressed quasiparticle bandstructure in accordance with results from Floquet-theory (pink lines). (a–c) Tr-APRES spectra for different amplitudes of resonant pump pulses showing hybridization between photon-dressed bands and equilibrium bands. With decreasing amplitude the hybridization gap also decreases. (d) At off-resonant pumping with energy smaller than the bandgap only photon-dressed replicas of valence bands occur within the gap. (e) Pumping with energy larger than the bandgap leads to a complex quasiparticle bandstructure with multiple interactions of photon-dressed bands with equilibrium bands.

properties to create a dressed-quasiparticle structure with a distinct valley and spin dependence.

We simulate the pump–probe photoemission process and angle resolved measurement where the pump is a circularly polarized monochromatic pulse that is long enough to drive the electronic structure into a nonequilibrium but stationary state, which usually is a few cycles of a field with  $\sim 1$  eV. Then the probe is applied with typically a higher photon energy that is large enough to ionize electrons from the sample, here we use a UV pulse with  $\omega_p = 40$  eV. The fast oscillating probe field has an envelop of  $\sim 85$  fs, so that during the probing process the driving field completes several tenths of cycles. Thus, the measurement process effectively averages the oscillating nonequilibrium state over many of its cycles. The atomic structure of monolayer  $\text{WSe}_2$ , is depicted in Figure 1a, along with the Brillouin zone and the path across the  $K$  point that we are considering here. The observed photoelectron spectrum depends strongly on the overlap of the pump and probe pulses as shown in Figure 1c. When the two pulses do not overlap one only measures the equilibrium bandstructure of  $\text{WSe}_2$  but in case of overlapping pulses extra features occur in the spectrum. The nonequilibrium state of the driven monolayer consists of quasiparticles that are a combination of electrons from the material and photons from the driving field, so-called photon-dressed electronic states. Thus, the photon-dressed features rely on the fact that the pump and probe pulses are overlapping, while most commonly tr-ARPES measurements are used to probe the electron dynamics following an excitation and to monitor its decay dynamics.

The dressing of the electronic bands leads to replicas of the equilibrium bands shifted by the photon energy. In a simple noninteracting picture this would result in a bandstructure with copies of all bands shifted from the equilibrium position by the pump energy. However, under interacting conditions when the replica of a band is shifted such that it gets close to another equilibrium band the two can hybridize as schematically shown in Figure 1b. In particular, when the pump frequency has the energy of the bandgap, then replicas of the valence band top are moved to the conduction band bottom and vice versa. These dressed bands are directly observable in the ARPES spectra of Figure 1c. When the temporal overlap between pump and probe pulse is modified, we can observe how the dressed bands collapse to the equilibrium bands. This means it is possible to directly observe the creation and destruction of the photon-

electron quasiparticle by tuning the pump–probe overlap: the real-time dressing and undressing of an electron.

**Floquet Theory.** The observed quasiparticle structure can be understood in terms of Floquet theory,<sup>34,35</sup> where a stationary state is expanded into a basis of Fourier components of multiples of the photon frequency  $\Omega$ :  $|\psi(t)\rangle = \sum_m \exp(-i(\varepsilon + m\Omega)t)|u_m\rangle$ , where  $\varepsilon$  is a quasi-static energy level. With this ansatz the time-dependent Schrödinger equation becomes an eigenvalue problem  $\sum_n \mathcal{H}^{mn}|u_n\rangle = \varepsilon|u_m\rangle$  of the static Floquet Hamiltonian  $\mathcal{H}^{mn} = \frac{\Omega}{2\pi} \int_{2\pi/\Omega} dt e^{i(m-n)\Omega t} H(t) + \delta_{mn}m\Omega$ . The eigenstates of this Hamiltonian span a Hilbert space with the dimension of the original electronic Hilbert space times the multiphoton dimension. The contribution of the latter is in principle infinite but here can be truncated. The spectrum of this Hamiltonian gives the bandstructure of the dressed quasiparticles. We compute the Floquet bandstructure using Floquet-TDDFT<sup>12</sup> where the time-dependent Hamiltonian of TDDFT is used in the Floquet analysis described above. We point out that we do not perform a high-frequency expansion, but rather restrict the Floquet Hamiltonian to contain only  $\pm\Omega$  terms.

In Figure 1c are also shown, side-by-side with the calculated ARPES spectra, the Floquet bands corresponding to the pump parameters used in the ARPES simulation. The dressed bands observed in the ARPES calculation are perfectly reproduced. We note that only certain bands hybridize while others make clean crossings. This is due to the spin polarization of the states and will be discussed below in more detail. Here we would like to point out the core finding of the work: the dressed states can be interpreted as Floquet-sidebands and the measurement process in ARPES with a finite-width probe pulse can in turn be interpreted as performing a time average of the nonequilibrium oscillating electronic structure corresponding to the time integrals in the Floquet analysis. In particular, the undressing process can be described in terms of a Floquet bandstructure with an effective constant amplitude, despite the fact that the amplitude is actually varying over the time during which the probe is applied. The undressing occurs while the pump is being switched off and thus the amplitude is actually changing while the system is probed by the finite probe pulse. This means that the system is not strictly a time-periodic stationary state. However, the tr-ARPES bandstructure computed under this condition perfectly agrees with the Floquet bandstructure

that by definition assumes a constant pumping amplitude and thus is strictly speaking not applicable to this situation because it represents a transient state. In the case of Figure 1c, the effective amplitude that reproduces the switching-off bandstructure corresponds to the amplitude of the shaped pump pulse at the time where the center of the probe pulse is located. Again, we point out that these two matching bandstructures are obtained independently with two different computational approaches. This underlines how the Floquet expansion is not only the correct way to describe the time-averaging inherent in a probe measurement but that it is also applicable even when the system is not strictly stationary. Clearly, this is only the case when the transient components of the oscillation are small and therefore the error committed in using Floquet analysis is small. For faster changing nonequilibrium states, this will certainly break down.

**Scaling.** Varying the amplitude and energy of the pump pulse leads to characteristic scaling behavior of the interaction between photon-dressed and equilibrium bands. Figure 2 shows that when the energy of the pump-pulse is in resonance with the bandgap the photon-dressed states hybridize with both the equilibrium valence and conduction bands, where the amount of the hybridization depends on the amplitude of the pump pulse. When the pump energy is smaller than the bandgap the tr-ARPES spectrum shows only replicas of the valence bands in the bandgap and no hybridization is discernible. For pump energies larger than the bandgap, however, there are multiple avoided crossings of different photon-dressed bands indicating a complex interaction between the different states.

Now, using results from Floquet theory we can systematically elucidate this behavior. Figure 3a shows the energy shift of the top valence band at  $K$  as a function of the amplitude for different pump energies. We observe that there is qualitative difference between the resonant and those pumps that are detuned from the band gap. While in the resonant case the shift grows linearly with the amplitude, detuning initially leads to a quadratic onset and only for large amplitudes a linear behavior is observed. This different scaling behavior can be rationalized by considering a simple driven two level model system with the Hamiltonian

$$H(t) = \frac{\epsilon}{2}(|c\rangle\langle c| - |v\rangle\langle v|) + (M|v\rangle\langle c| + c. g. )A \cos(\Omega t) \quad (1)$$

where,  $\epsilon$  is the energy gap,  $M = \langle v|rc\rangle$  is the dipole matrix element between the two states, and  $A$  the amplitude of the driving field. Constructing the Floquet Hamiltonian for this system while considering only one-photon interactions, further restricting it to one-photon absorption (see Supporting Information) and diagonalizing it, gives the shift of the levels as a function of amplitude and frequency of the pump laser as  $\Delta E = \sqrt{A^2|M|^2 + (\Omega - \epsilon)^2}$ . When  $\Omega$  is in resonance with the gap,  $\Omega \rightarrow \epsilon$ , this shift simplifies to  $\Delta E_{\text{res}} = A|M|$ , that is, it grows linearly as a function of the field intensity. In case of detuning,  $\Omega \rightarrow \epsilon + \delta$ , the energy shift is  $\Delta E_{\text{det}} = \sqrt{A^2|M|^2 + \delta^2}$ . Expanding this for small amplitudes gives  $\Delta E_{\text{det}} \approx \delta + \frac{A^2|M|^2}{2\delta}$ . Thus, for off-resonant driving and  $A|M| \ll \delta$  the energy shift grows quadratically with the amplitude, as observed in Figure 3a.

**Optical Stark Effect.** In fact, a quadratic dependence on the amplitude of a light-induced energy shift is the well-known

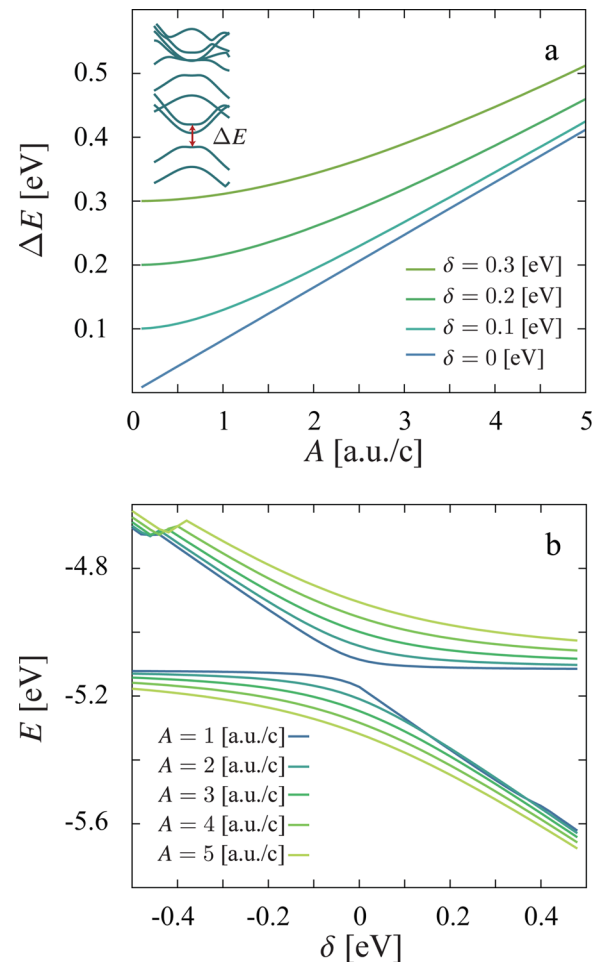


**Figure 3.** Scaling behavior of hybridization induced energy shift with laser parameters  $A$  and  $\delta$ . (a) Using the bandstructures resulting from Floquet theory the scaling of the hybridization gap (see main text for a discussion) between the photon-dressed conduction band minimum and the valence band top (inset) is shown as a function of the pump laser amplitude for different detuning energies, behaving quadratically as expected from the ac-Stark effect. (b) The hybridization gap of (a) can be seen as an avoided crossing of the two bands when scanning the pump energy through the resonance with the bandgap.

behavior the optical Stark effect<sup>36</sup> that emerges thus naturally from Floquet theory. This highlights the fact that the dressed bands observed in the ARPES calculation are the underlying electronic structure of the optical Stark effect. In particular, in a recent experiment Sie et al.<sup>22</sup> demonstrate a valley selective optical Stark effect in a transition metal dichalcogenide with an all optical pump–probe measurement. Here, we can discuss this experiment in terms of the underlying electronic quasiparticle process, as it is accessible through ARPES and provide a detailed picture of how the optical Stark effect occurs on the level of the electronic structure.

Monolayer  $\text{WSe}_2$  is known to have circular pump dichroism,<sup>37</sup> originating from a well-defined angular momentum character of electronic orbitals at the  $K$  and  $K'$  points in the Brillouin zone.<sup>38</sup> Thus, a dipole selection rule determines that for a given circularly polarized pump the electronic density at only one of the two  $K$  valleys is excited. Figure 4 shows how pumping with left-handed circularly polarized light results in the formation of photon-dressed bands only in the  $K$ -valley and thus in a valley selective optical Stark effect. The hybridization

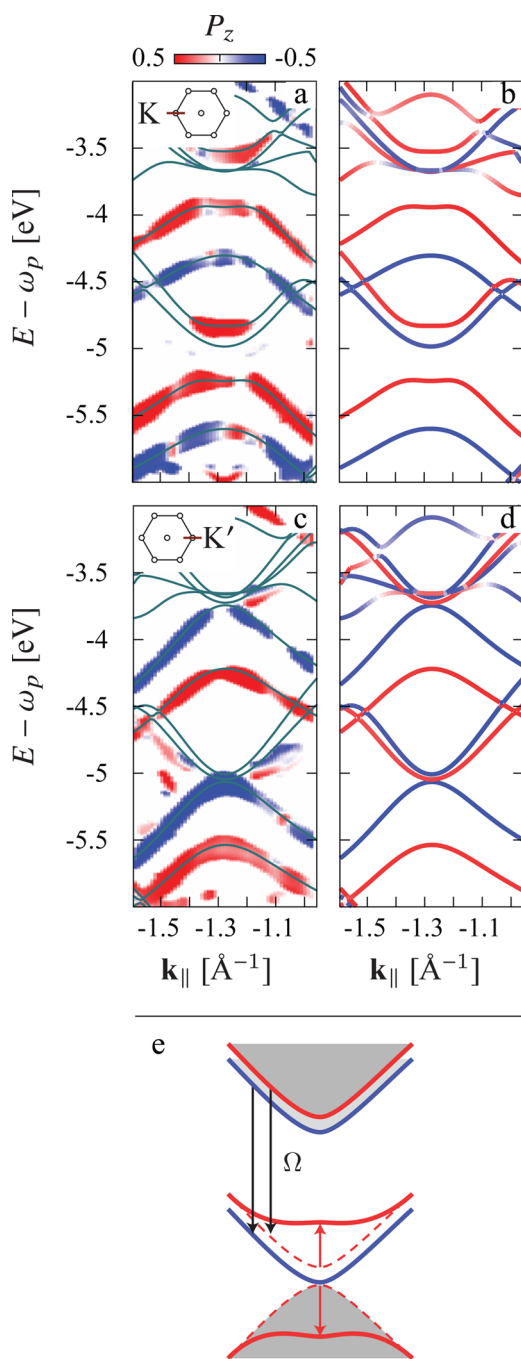


**Figure 4.** Dichroic optical Stark effect. Spin polarization of the photodressed bands obtained with tr-ARPES (panel a (c)) and Floquet theory (panel b (d)) at K (K'). (e) The photodressed states hybridize with bands that are close in energy but only within the same spin polarization subspace.

of the bands leads to a down shift of the valence band and to an upshift of the conduction band and thus in an overall opening of the equilibrium band gap at the *K* valley. Also, there is a spin dependence of this process that would clearly manifest in a spin resolved tr-ARPES measurement. When electronic excitation is prevented by dipole matrix elements, only the valence bands appear as photon-dressed replicas in the photoemission spectrum while the absence of electronic population in the conduction bands implies that there are no electronic bands available to be dressed, as seen in Figure 4. Because the Stark effect is a result of the hybridization between photon-dressed

valence and conduction bands with the respective undressed bands, the absence of population in the conduction bands in the *K'*-valley precluding any hybridization thus implies that the Stark effect does not occur. In an optical absorption experiment, this selective gap opening is observable as a shift of the absorption peak<sup>22</sup> of circularly polarized light with the same helicity as the pump, whereas a probe with the opposite helicity only interacts with the unshifted bandstructure of the *K* valley that is unaffected by the circular pump.

Our calculation also elucidates the role of spin polarization in the observable Stark effect. The broken inversion symmetry of the monolayer with respect to the symmetric bulk phase leads to a spin–orbit splitting of the valence and conduction bands with a nearly perfect spin polarization of the two bands at *K*.<sup>32</sup> We have noted before that in the Floquet bandstructures in Figures 1 and 2 only certain bands appear to be hybridizing. From Figure 4 this effect becomes clear and can be identified to originate from the spin polarization of the equilibrium bands: the photon-dressed states inherit the spin polarization from the underlying equilibrium bandstructure and therefore the hybridization is spin selective, that is, only bands with the same spin polarization will hybridize, see Figure 4e. In particular, this means that a pump energy equal to the band gap does not actually move the photon-dressed states into perfect resonance because the states at the band edges have opposite spin polarization. Instead to achieve exact resonant condition the required energy is equal to the difference between a conduction and valence bands with the same spin polarization, as has been used in Figure 3a,b.

**Discussion.** The photon dressing of electrons to form nonequilibrium quasiparticles is the fundamental process underlying the vast amount of theoretical proposals in the rapidly developing field of Floquet-topological materials. Here we describe the conditions for the direct observation of such bands in a semiconducting monolayer TMD. We have discussed the role of the photon-dressed states in terms of the optical Stark effect but the Floquet quasiparticle structure of monolayer TMDs also hosts topological properties. In equilibrium, most monolayer TMDs are ordinary semiconductors but it has been recently proposed<sup>3</sup> that they can be driven by monochromatic light to form a Floquet-topological insulator. The energy of the protected edge states of such a nonequilibrium phase crosses the hybridization gap between the photon-dressed state and an equilibrium band and including an edge geometry in our calculation would show also this band. There is thus a direct connection between the bandstructure presented here and the Floquet topological phase. Our work shows by first-principles calculations that the measurement of the nonequilibrium bands with ARPES is intimately linked to the Floquet quasiparticle spectrum. Indeed, by using two completely independent computational methods we systematically obtain the same nonequilibrium bandstructures. We believe that this work paves the way to understanding the measurement of dynamical photon dressing phenomena in a large variety of materials in nonequilibrium phases.

## ■ ASSOCIATED CONTENT

### Supporting Information

The Supporting Information is available free of charge on the ACS Publications website at DOI: 10.1021/acs.nanolett.6b04419.

Derivation of the ac-Stark effect from Floquet theory (PDF)

## AUTHOR INFORMATION

### Corresponding Author

\*E-mail: [angel.rubio@mpsd.de](mailto:angel.rubio@mpsd.de).

### ORCID

Umberto De Giovannini: 0000-0002-4899-1304

### Author Contributions

U.D.G. and H.H. contributed equally to this work.

### Notes

The authors declare no competing financial interest.

## ACKNOWLEDGMENTS

We are grateful for illuminating discussions with M. Sentef and R. Ernstorfer. We acknowledge financial support from the European Research Council (ERC-2015-AdG-694097), Spanish Grant (FIS2013-46159-C3-1-P), Grupos Consolidados (IT578-13), AFOSR Grant FA2386-15-1-0006 AOARD 144088, and European Union Horizon 2020 Research and Innovation program under Grant Agreements 676580 (NOMAD) and 646259 (MOSTOPHOS). H.H. acknowledges support from the People Programme (Marie Curie Actions) of the European Union's Seventh Framework Programme FP7-PEOPLE-2013-IEF project No. 622934.

## REFERENCES

- (1) Faisal, F. H. M.; Kamiński, J. Z. *Phys. Rev. A: At., Mol., Opt. Phys.* **1997**, *56*, 748–762.
- (2) Lindner, N. H.; Refael, G.; Galitski, V. *Nat. Phys.* **2011**, *7*, 490–495.
- (3) Claassen, M.; Jia, C.; Moritz, B.; Devereaux, T. P. *Nat. Commun.* **2016**, *7*, 13074.
- (4) Sentef, M. A.; Claassen, M.; Kemper, A. F.; Moritz, B.; Oka, T.; Freericks, J. K.; Devereaux, T. P. *Nat. Commun.* **2015**, *6*, 7047.
- (5) Suarez Morell, E.; Foa Torres, L. E. F. *Phys. Rev. B: Condens. Matter Mater. Phys.* **2012**, *86*, 125449.
- (6) Kitagawa, T.; Oka, T.; Brataas, A.; Fu, L.; Demler, E. *Phys. Rev. B: Condens. Matter Mater. Phys.* **2011**, *84*, 235108.
- (7) Jiang, L.; Kitagawa, T.; Alicea, J.; Akhmerov, A. R.; Pekker, D.; Refael, G.; Cirac, J. I.; Demler, E.; Lukin, M. D.; Zoller, P. *Phys. Rev. Lett.* **2011**, *106*, 220402.
- (8) Li, Y.; Kundu, A.; Zhong, F.; Seradjeh, B. *Phys. Rev. B: Condens. Matter Mater. Phys.* **2014**, *90*, 121401.
- (9) Benito, M.; Gómez-León, A.; Bastidas, V. M.; Brandes, T.; Platero, G. *Phys. Rev. B: Condens. Matter Mater. Phys.* **2014**, *90*, 205127.
- (10) Liu, Z. K.; Zhou, B.; Zhang, Y.; Wang, Z. J.; Weng, H. M.; Prabhakaran, D.; Mo, S. K.; Shen, Z. X.; Fang, Z.; Dai, X.; Hussain, Z.; Chen, Y. L. *Science* **2014**, *343*, 864–867.
- (11) Ali, M. N.; Gibson, Q.; Jeon, S.; Zhou, B. B.; Yazdani, A.; Cava, R. J. *Inorg. Chem.* **2014**, *53*, 4062–4067.
- (12) Hübener, H.; Sentef, M. A.; De Giovannini, U.; Kemper, A. F.; Rubio, A. *Nat. Commun.* **2016**, *7*, 13940.
- (13) Zou, J.-Y.; Liu, B.-G. *Phys. Rev. B: Condens. Matter Mater. Phys.* **2016**, *93*, 205435.
- (14) Wang, H.; Zhou, L.; Chong, Y. D. *Phys. Rev. B: Condens. Matter Mater. Phys.* **2016**, *93*, 144114.
- (15) Yan, Z.; Wang, Z. *Phys. Rev. Lett.* **2016**, *117*, 087402.
- (16) Chan, C.-K.; Oh, Y.-T.; Han, J. H.; Lee, P. A. *Phys. Rev. B: Condens. Matter Mater. Phys.* **2016**, *94*, 121106.
- (17) Hsu, H.; Reichl, L. E. *Phys. Rev. B: Condens. Matter Mater. Phys.* **2006**, *74*, 115406.
- (18) Fleury, R.; Khanikaev, A. B.; Alù, A. *Nat. Commun.* **2016**, *7*, 11744.
- (19) Wang, Y. H.; Steinberg, H.; Jarillo-Herrero, P.; Gedik, N. *Science* **2013**, *342*, 453–457.
- (20) Mahmood, F.; Chan, C.-K.; Alpichshev, Z.; Gardner, D.; Lee, Y.; Lee, P. A.; Gedik, N. *Nat. Phys.* **2016**, *12*, 306–310.
- (21) Autler, S. H.; Townes, C. H. *Phys. Rev.* **1955**, *100*, 703–722.
- (22) Sie, E. J.; McIver, J. W.; Lee, Y.-H.; Fu, L.; Kong, J.; Gedik, N. *Nat. Mater.* **2014**, *14*, 290–294.
- (23) Runge, E.; Gross, E. K. U. *Phys. Rev. Lett.* **1984**, *52*, 997–1000.
- (24) De Giovannini, U.; Varsano, D.; Marques, M. A. L.; Appel, H.; Gross, E. K. U.; Rubio, A. *Phys. Rev. A: At., Mol., Opt. Phys.* **2012**, *85*, 062515–14.
- (25) Wopperer, P.; De Giovannini, U.; Rubio, A. 2016, <https://arxiv.org/abs/1608.02818> (accessed Nov 29, 2016).
- (26) De Giovannini, U.; Hübener, H.; Rubio, A. 2016, <http://arxiv.org/abs/1609.03092> (accessed Nov 29, 2016).
- (27) Kristinsson, K.; Kibis, O. V.; Morina, S.; Shelykh, I. A. *Sci. Rep.* **2016**, *6*, 20082.
- (28) Pervishko, A. A.; Kibis, O. V.; Morina, S.; Shelykh, I. A. *Phys. Rev. B: Condens. Matter Mater. Phys.* **2015**, *92*, 205403.
- (29) Morina, S.; Kibis, O. V.; Pervishko, A. A.; Shelykh, I. A. *Phys. Rev. B: Condens. Matter Mater. Phys.* **2015**, *91*, 155312.
- (30) Xu, X.; Yao, W.; Xiao, D.; Heinz, T. F. *Nat. Phys.* **2014**, *10*, 343–350.
- (31) Zhang, X.; Liu, Q.; Luo, J.-W.; Freeman, A. J.; Zunger, A. *Nat. Phys.* **2014**, *10*, 387–393.
- (32) Riley, J. M.; Mazzola, F.; Dendzik, M.; Michiardi, M.; Takayama, T.; Bawden, L.; Granerod, C.; Leandersson, M.; Balasubramanian, T.; Hoesch, M.; et al. *Nat. Phys.* **2014**, *10*, 835–839.
- (33) Bertoni, R.; Nicholson, C. W.; Waldecker, L.; Hübener, H.; Monney, C.; de Giovannini, U.; Puppini, M.; Hoesch, M.; Springate, E.; Chapman, R. T.; Cacho, C.; Wolf, M.; Rubio, A.; Ernstorfer, R. 2016, <http://arxiv.org/abs/1606.03218> (accessed Nov 29, 2016).
- (34) Sambe, H. *Phys. Rev. A: At., Mol., Opt. Phys.* **1973**, *7*, 2203–2213.
- (35) Hone, D. W.; Ketzmerick, R.; Kohn, W. *Phys. Rev. A: At., Mol., Opt. Phys.* **1997**, *56*, 4045–4054.
- (36) Sussman, B. J. *Am. J. Phys.* **2011**, *79*, 477.
- (37) Cao, T.; Wang, G.; Han, W.; Ye, H.; Zhu, C.; Shi, J.; Niu, Q.; Tan, P.; Wang, E.; Liu, B.; Feng, J. *Nat. Commun.* **2012**, *3*, 887.
- (38) Berghäuser, G.; Malic, E. *Phys. Rev. B: Condens. Matter Mater. Phys.* **2014**, *89*, 125309–6.